Finite element dynamic analysis of laminated composite beams under moving loads

Volkan Kahya*

Department of Civil Engineering, Karadeniz Technical University, 61080 Trabzon, Turkey

Abstract. This study presents dynamic analysis of laminated beams traversed by moving loads using a multilayered beam element based on the first-order shear deformation theory. The present element consists of N layers with different thickness and material property, and has $(3N + 7)$ degrees of freedom corresponding three axial, four transversal, and $3N$ rotational displacements. Delamination and interfacial slip are not allowed. Comparisons with analytical and/or numerical results available in literature for some illustrative examples are made. Numerical results for natural frequencies, deflections and stresses of laminated beams are given to explain the effect of load speed, lamina layup, and boundary conditions.

Keywords: moving loads; laminated beams; multilayered beam element; first-order shear deformation theory; finite element method

1. Introduction

Use of fiber-reinforced polymer composites in bridge engineering is tremendously increased since they can be alternative to conventional bridge construction materials due to their merits, such as low density, high strength, long-term durability, and good corrosion and fatigue resistance.

Bridges are designed to carry moving traffic loads in addition to their self-weight. It is well known moving loads cause greater deflections and stresses than those due to static loads. Thus, dynamic nature of moving loads must be considered in bridge design and analysis. Extensive experimental and theoretical research on dynamic response of bridges modeled as an isotropic beam or a plate structure has been carried out (Hino *et al.* 1984, Frýba 1999, Au *et al.* 2000, Yang *et al.* 2004, Abu-Hilal and Mohsen 2006, Kocatürk and Şimşek 2006, Şimşek and Kocatürk 2009, Cantero *et al.* 2010).

Response of laminated composite and sandwich structures to moving loads has been, however, rarely studied. Chonan (1987) studied steady state response of thick sandwich strip plate to moving line load of constant magnitude. The problem was studied on the basis of a thick plate theory and the solution is obtained by applying the method of the complex Fourier transform. Based on the higher-order shear deformation theory, Kadivar and Mohebpour (1998) derived a laminated beam element including Poisson effect and bend-stretch, shear-stretch, and bend-twist couplings to analyze moving load-induced vibrations of unsymmetric laminated composite beams. Stochastic vibrations

---

*Corresponding author, Assistant Professor, E-mail: volkan@ktu.edu.tr

of laminated composite coated beams traversed by a moving random load were studied by Zibdeh and Abu-Hilal (2003). They assumed the load moving with accelerating, decelerating and constant velocity types of motion. Kiral *et al.* (2004) investigated dynamic behavior of laminated composite beams under moving loads using a three-dimensional finite element model based on classical lamination theory. Lee *et al.* (2004) examined the dynamic behavior of single and two-span continuous composite plates subjected to multi-moving loads. Their finite element formulation was based on the third-order shear deformation theory and considered the rotary inertia. Kavipurapu (2005) studied the dynamic response of simply supported glass/epoxy composite beams subjected to moving loads in a hygrothermal environment. Malekzadeh *et al.* (2009) presented a solution procedure based on three-dimensional elasticity theory to determine the dynamic response of cross-ply laminated thick plates under moving loads. Ghafoori and Asghari (2010) investigated dynamic response of angle-ply laminated composite plates traversed by a moving mass or a moving force. Based on the first-order shear deformation theory, they derived a rectangular plate element using adaptive finite element method. Kahya and Mosallam (2011) considered the moving mass problem of composite sandwich beams to study effects of vehicle mass, vehicle speed, fiber orientation and lamina thickness on the beam response and the contact force at the mass-beam interface. An algorithm based on the finite element method was developed by Mohebpour *et al.* (2011a, b) to study the dynamic response of laminated composites subjected to moving oscillators. Recently, Kahya (2012) studied laminated composite beams under moving loads using a multilayered beam element developed by Yuan and Miller (1989) based on the first-order shear deformation theory.

This study extends the author's previous work (Kahya 2012) to present comprehensive results for dynamic response of laminated beams to moving loads. The present beam element includes separate rotational degrees of freedom for each lamina without any additional axial and transversal degrees of freedom beyond those necessary for a single lamina. Formulation is based on the first-order shear deformation theory. The shape functions are selected to ensure compatibility between the laminae. Interfacial slip and delamination are not allowed.

2. Governing equations

As shown in Fig. 1, a point load P moves on a laminated beam with a constant speed c. The beam consists of N-stacked laminae. Each lamina may have its own thickness and material properties. Governing differential equations for this problem can be written as

$$
\begin{aligned}
EAu'' - m\ddot{u} &= 0 \\
KGA(v'' - \phi') - m\ddot{v} + p(x, t) &= 0 \\
EI\phi'' + KGA(v' - \phi) - \rho I\ddot{\phi} &= 0
\end{aligned}
\tag{1}
$$

where $u(x,t), v(x,t)$, and $\phi(x,t)$ denote axial, transversal and rotational displacements, respectively. m is mass per unit length, E is Young's modulus, G is shear modulus, A is cross-sectional area, I is second moment of area, ρ is mass density of the beam, and K is shear correction factor which is taken as 5/6 for a rectangular cross-section. Prime and over dot denote the derivatives with respect to x and t, respectively. For a concentrated load moving on the beam, the load function $p(x, t)$ can be defined as

$$p(x,t) = P\delta(x - ct) \tag{2}$$

where P and c denote magnitude and speed of the moving load, respectively. $\delta(\cdot)$ is Dirac delta function.

3. Finite element formulation

3.1 Single lamina element

The single lamina element for constitution of multilayered beam element has five nodes as shown in Fig. 2. It includes 10-degrees of freedom that are three axial, four transversal and three rotational displacements, respectively. All nodal displacements are measured at midplane of the lamina.

Solutions to $u(x,t), v(x,t)$, and $\phi(x,t)$ can be assumed as

$$u(x,t) = \sum_{i=1}^{3} \varphi_i(x)u_i(t), \quad v(x,t) = \sum_{i=1}^{4} \psi_i(x)v_i(t), \quad \phi(x,t) = \sum_{i=1}^{3} \theta_i(x)\phi_i(t) \tag{3}$$

where $\phi_i(x)$, $\psi_i(x)$ and $\theta_i(x)$ are shape functions, and $u_i(t), v_i(t)$ and $\phi_i(t)$ are generalized nodal displacements. Quadratic polynomials for $\varphi_i(x)$ and $\theta_i(t)$, and a cubic polynomial for $\psi_i(x)$ are selected for consistency as explained in Yuan and Miller (1989) and Kahya (2012).

Using Galerkin-weighted residual approach, and following the usual procedure of the finite element method (Zienkiewicz and Taylor 2000), equation of motion of the single lamina element can be written as
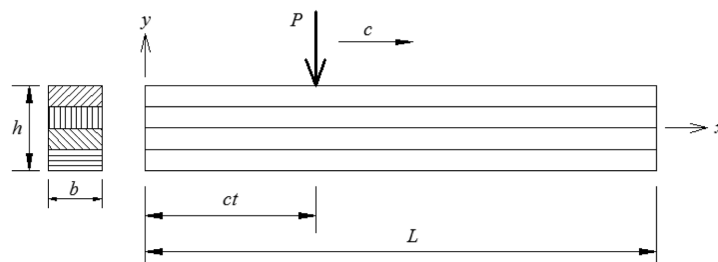
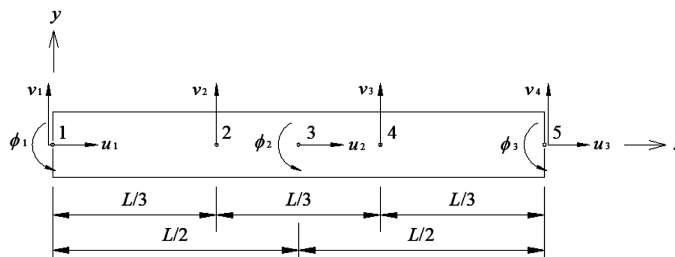Fig. 1 Geometry and dimensions of a laminated beam traversed by a moving point load

Fig. 2 10-degrees of freedom single lamina element

$$\mathbf{m\ddot{u}} + \mathbf{ku} = \mathbf{f} \tag{4}$$

where **m**, **k**, **f** and **u** denote element mass matrix, element stiffness matrix, nodal load vector and nodal displacements vector, respectively, and are defined as

$$\mathbf{m} = \begin{bmatrix} \mathbf{m}^{11} & \mathbf{0} & \mathbf{0} \\ \mathbf{0} & \mathbf{m}^{22} & \mathbf{0} \\ \mathbf{0} & \mathbf{0} & \mathbf{m}^{33} \end{bmatrix}, \quad \mathbf{k} = \begin{bmatrix} \mathbf{k}^{11} & \mathbf{0} & \mathbf{0} \\ \mathbf{0} & \mathbf{k}^{22} & \mathbf{k}^{23} \\ \mathbf{0} & \mathbf{k}^{23T} & \mathbf{k}^{33} \end{bmatrix}, \quad \mathbf{f} = \{\mathbf{0}\ \mathbf{f}^2\ \mathbf{0}\}^T \tag{5}$$

where

$$m_{ij}^{11} = \int_0^{L_e} m\,\varphi_i\varphi_j dx \quad (i,j=1-3), \quad m_{ij}^{22} = \int_0^{L_e} m\,\psi_i\psi_j dx \quad (i,j=1-4)$$

$$m_{ij}^{33} = \int_0^{L_e} \rho I\theta_i\theta_j dx \quad (i,j=1-3), \quad k_{ij}^{11} = \int_0^{L_e} EA\varphi_i'\varphi_j' dx \quad (i,j=1-3)$$

$$k_{ij}^{22} = \int_0^{L_e} KGA\psi_i'\psi_j' dx \quad (i,j=1-4), \quad k_{ij}^{23} = -\int_0^{L_e} KGA\psi_i'\theta_j dx \quad (i=1-4, j=1-3)$$

$$k_{ij}^{33} = \int_0^{L_e} (EI\theta_i'\theta_j' + KGA\theta_i\theta_j)dx \quad (i,j=1-3), \quad f_i^2 = P\psi_i(ct) \quad (i=1-4) \tag{6}$$

where L_e is the element length. **m** and **k** matrices are given in Kahya (2012) explicitly.

3.2. Multilayered beam element

Multilayered beam element consists of *N*-stacked laminae as shown in Fig. 3. When constituting multiple laminae, only rotational degrees of freedom are added to the system. No additional axial and transversal degrees of freedom are necessary. Consequently, for *N*-layer beam element, total number of degrees of freedom is $(3N+7)$. To constitute the mass and stiffness matrices of multilayered beam element, the following procedure is employed (Yuan and Miller 1989).

According to Eq. (4), the load-displacement relations for each lamina can be written as

$$\mathbf{f}^{(N)} = \mathbf{m}^{(N)}\ddot{\mathbf{X}}^{(N)} + \mathbf{k}^{(N)}\mathbf{X}^{(N)}$$

$$\mathbf{f}^{(N-1)} = \mathbf{m}^{(N-1)}\ddot{\mathbf{X}}^{(N-1)} + \mathbf{k}^{(N-1)}\mathbf{X}^{(N-1)}$$

$$\vdots$$

$$\mathbf{f}^{(1)} = \mathbf{m}^{(1)}\ddot{\mathbf{X}}^{(1)} + \mathbf{k}^{(1)}\mathbf{X}^{(1)} \tag{7}$$

where $\mathbf{f}^{(i)}$ denotes the nodal force vector, and $\mathbf{X}^{(i)}$ is a column vector including the local variables of *i*th lamina as well as the rotational variables of the other laminae between *i* and *N*, and has dimension $(10+3N-3i)\times 1$.

The local displacement vector $\mathbf{u}^{(i)}$ for each lamina can be converted to $\mathbf{X}^{(i)}$ by using (Yuan and Miller 1989)
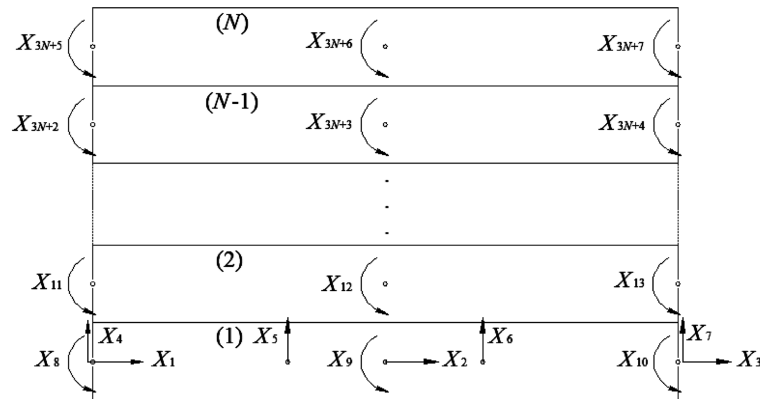
Fig. 3 Multilayered beam element

$$\mathbf{u}^{(N)} = \mathbf{R}^{(N)}\mathbf{X}^{(N)}$$
$$\mathbf{u}^{(N-1)} = \mathbf{R}^{(N-1)}\mathbf{X}^{(N-1)}$$
$$\vdots$$
$$\mathbf{u}^{(1)} = \mathbf{R}^{(1)}\mathbf{X}^{(1)}$$

$$(8)$$

where $\mathbf{R}^{(i)}$ is a $10 \times (10 + 3N - 3i)$ matrix defined as

$$\text{All} \quad R_{jk}^{(i)} = 0 \quad \text{except} \quad R_{jj}^{(i)} = 1 \quad (j = 1 - 10) \tag{9}$$

$\mathbf{X}^{(i)}$ vector can be converted to $\mathbf{X}^{(i-1)}$ by the following relations (Yuan and Miller 1989).

$$\mathbf{X}^{(N)} = \mathbf{T}^{(N-1)}\mathbf{X}^{(N-1)}$$
$$\mathbf{X}^{(N-1)} = \mathbf{T}^{(N-2)}\mathbf{X}^{(N-2)}$$
$$\vdots$$
$$\mathbf{X}^{(2)} = \mathbf{T}^{(1)}\mathbf{X}^{(1)}$$

$$(10)$$

where $\mathbf{T}^{(i)}$ is a $(7 + 3N - 3i) \times (10 + 3N - 3i)$ matrix defined as

$$\text{All} \quad T_{jk}^{(i)} = 0 \quad \text{except} \quad T_{j(j+7)}^{(i)} = -h^{(i)}/2, \quad T_{j(j+10)}^{(i)} = -h^{(i+1)}/2 \quad (j = 1 - 3)$$
$$T_{jj}^{(i)} = 1 \quad (j = 1 - 7)$$
$$T_{j(j+3)}^{(i)} = 1 \quad (j = 8 - (7 + 3N - 3i)) \tag{11}$$

In order to transform the local load vectors given by Eq. (7) to the global ones, the followings can be used (Yuan and Miller 1989).

$$\mathbf{F}^{(1)} = \mathbf{R}^{(1)^T}\mathbf{f}^{(1)}$$

$$\mathbf{F}^{(2)} = \mathbf{T}^{(1)^T}\mathbf{R}^{(2)^T}\mathbf{f}^{(2)}$$

$$\vdots$$

$$\mathbf{F}^{(N)} = \mathbf{T}^{(1)^T}\mathbf{T}^{(2)^T}\cdots\mathbf{T}^{(N-1)^T}\mathbf{R}^{(N)^T}\mathbf{f}^{(N)} \tag{12}$$

Combining Eqs. (7) to (12) together gives the final expressions for the stiffness and mass matrices of the multilayered beam element as follows (Bassiouni *et al.* 1999, Kahya 2012).

$$\mathbf{K}^e = \mathbf{R}^{(1)^T}\mathbf{k}^{(1)}\mathbf{R}^{(1)} + \mathbf{T}^{(1)^T}(\mathbf{R}^{(2)^T}\mathbf{k}^{(2)}\mathbf{R}^{(2)} + \mathbf{T}^{(2)^T}(\mathbf{R}^{(3)^T}\mathbf{k}^{(3)}\mathbf{R}^{(3)} + \dots$$

$$+ \mathbf{T}^{(N-2)^T}(\mathbf{R}^{(N-1)^T}\mathbf{k}^{(N-1)}\mathbf{R}^{(N-1)} + \mathbf{T}^{(N-1)^T}\mathbf{k}^{(N)}\mathbf{T}^{(N-1)}\mathbf{T}^{(N-2)})\dots)\mathbf{T}^{(2)})\mathbf{T}^{(1)} \tag{13}$$

$$\mathbf{M}^e = \mathbf{R}^{(1)^T}\mathbf{m}^{(1)}\mathbf{R}^{(1)} + \mathbf{T}^{(1)^T}(\mathbf{R}^{(2)^T}\mathbf{m}^{(2)}\mathbf{R}^{(2)} + \mathbf{T}^{(2)^T}(\mathbf{R}^{(3)^T}\mathbf{m}^{(3)}\mathbf{R}^{(3)} + \dots$$

$$+ \mathbf{T}^{(N-2)^T}(\mathbf{R}^{(N-1)^T}\mathbf{m}^{(N-1)}\mathbf{R}^{(N-1)} + \mathbf{T}^{(N-1)^T}\mathbf{m}^{(N)}\mathbf{T}^{(N-1)}\mathbf{T}^{(N-2)})\dots)\mathbf{T}^{(2)})\mathbf{T}^{(1)} \tag{14}$$

The equation of motion of the laminated beam in terms of Xs can thus be written as follows

$$\mathbf{M}\ddot{\mathbf{X}} + \mathbf{K}\mathbf{X} = \mathbf{F} \tag{15}$$

where $\mathbf{M}$ and $\mathbf{K}$ are the system mass and stiffness matrices, and $\mathbf{F}$ is the nodal force vector, respectively. After imposing the boundary conditions, the system equations given by Eq. (15) will be solved numerically by using the Newmark's method. Note that the nodal force vector contains zeroes for all degrees of freedom except those corresponding to the transverse displacements in the element on which the moving load acts.

3.3 Stresses in laminated beams

Finite element stress locations are shown in Fig. 4 for a single lamina. The normal and shear stresses will be calculated according to the Hooke's law, i.e., $\sigma_x = E\varepsilon_x$ and $\tau_{xy} = G\gamma_{xy}$, where $\varepsilon_x = \partial u/\partial x$ and $\gamma_{xy} = \partial u/\partial y + \partial v/\partial x$ are the axial and shear strains, respectively. With the degrees of freedom provided by the present element, the normal stress σ_x has a linear variation through thickness while the shear stress τ_{xy} is constant.

Substituting Eq. (3) into the strain expressions, after some manipulations, the following matrix equation can be obtained for stresses.

$$\sigma = \mathbf{H}\mathbf{X} \tag{16}$$

where $\mathbf{H}$ is a 6×10 matrix given in the Appendix, $\mathbf{X}$ contains the local variables of the single lamina, and σ is given by

$$\sigma = \{\sigma_L^+ \quad \sigma_L^- \quad \tau_L \quad \sigma_R^+ \quad \sigma_R^- \quad \tau_R\}^T \tag{17}$$
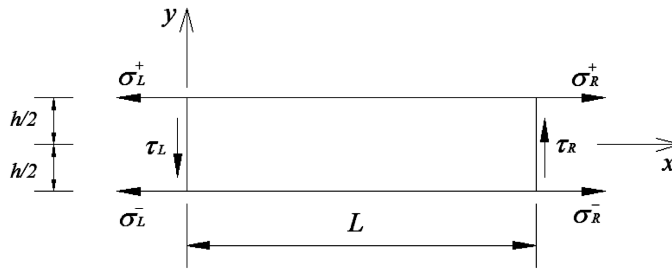
Fig. 4 Finite element stress locations for a single lamina

For an *N*-layer beam element, the equations for stresses in each lamina can be obtained by combining Eqs. (16), (8) and (10) as in the following.

$$\boldsymbol{\sigma}^{(N)} = \mathbf{H}^{(N)}\mathbf{R}^{(N)}\mathbf{T}^{(N-1)}\mathbf{T}^{(N-2)}...\mathbf{T}^{(1)}\mathbf{X} = \mathbf{Q}^{(N)}\mathbf{X}$$

$$\boldsymbol{\sigma}^{(N-1)} = \mathbf{H}^{(N-1)}\mathbf{R}^{(N-1)}\mathbf{T}^{(N-2)}\mathbf{T}^{(N-3)}...\mathbf{T}^{(1)}\mathbf{X} = \mathbf{Q}^{(N-1)}\mathbf{X}$$

$$\vdots$$

$$\boldsymbol{\sigma}^{(2)} = \mathbf{H}^{(2)}\mathbf{R}^{(2)}\mathbf{T}^{(1)}\mathbf{X} = \mathbf{Q}^{(2)}\mathbf{X}$$

$$\boldsymbol{\sigma}^{(1)} = \mathbf{H}^{(1)}\mathbf{R}^{(1)}\mathbf{X} = \mathbf{Q}^{(1)}\mathbf{X} \tag{18}$$

where $\mathbf{X} = \mathbf{X}^{(1)}$ has dimension $(3N+7) \times 1$.

4. Numerical results

4.1 Verification of the present model

Some numerical examples are first given to verify the present model. Based on the approach described above, a FORTRAN program is developed for numerical computations. The results obtained are compared with the analytical and/or numerical results available in literature for most cases. In all analyses, eight elements are used in finite element discretization along the beam length. Since the present element does not consider bending-stretching coupling, only cross-ply laminates and isotropic beams are taken into consideration.

Example 1   As a first example, an isotropic simply supported beam under center point load with magnitude P is considered since its analytical solution can be easily obtained. Material properties are $E = 206.8$ GPa, $\nu = 0.3$, and $\rho = 10686.9$ kg/m³. Table 1 shows the normalized maximum static deflections $\bar{v}$ and fundamental frequencies $\bar{\omega}$ for $L/h = 5$, 10 and 100. The followings are used for normalization

$$\bar{v} = 100\frac{\nu EAh^2}{PL^3}, \quad \bar{\omega} = \omega(L^2/h)\sqrt{\rho/E} \tag{19}$$

Comparisons with analytical solutions based on the Euler-Bernoulli and Timoshenko beam theories show the present model is quite successful to determine the static beam deflections, and

Table 1 Maximum static deflections $\bar{v}$ and fundamental frequencies $\bar{\omega}$ for a simply supported isotropic beam

L/h	NL	Model	$\bar{v}$	$\bar{\omega}$
5	1	Present	28.1200	2.6772
		EBT[1]	25.0000	2.8491
		TBT	28.1200	2.6772
	3	Present	28.4129	2.5631
		EBT	25.0075	2.8487
		TBT	28.1278	2.6768
	5	Present	28.5889	2.5100
		EBT	25.0000	2.8491
		TBT	28.1200	2.6772
10	1	Present	25.7800	2.8024
		EBT	25.0000	2.8491
		TBT	25.7800	2.8023
	3	Present	25.8612	2.7691
		EBT	25.0075	2.8487
		TBT	25.7876	2.8019
	5	Present	25.9005	2.7543
		EBT	25.0000	2.8491
		TBT	25.7800	2.8023
100	1	Present	25.0078	2.8487
		EBT	25.0000	2.8491
		TBT	25.0078	2.8486
	3	Present	25.0161	2.8480
		EBT	25.0075	2.8487
		TBT	25.0153	2.8482
	5	Present	25.0090	2.8482
		EBT	25.0000	2.8491
		TBT	25.0078	2.8486

[1]EBT – Euler-Bernoulli beam theory, TBT – Timoshenko beam theory

natural frequencies. As expected, shear deformation is important especially for thicker beams. Increase in the number of layers (NL) through the thickness does not cause any significant change on the results. Even only one layer is used, the present model gives good results for deflections and natural frequencies of isotropic beams.

Figs. 5 and 6 show the maximum normal and shear stress distributions through the thickness of the beam. To avoid the effect of shear, very slender beam ($L/h = 100$) is considered. Eight layers
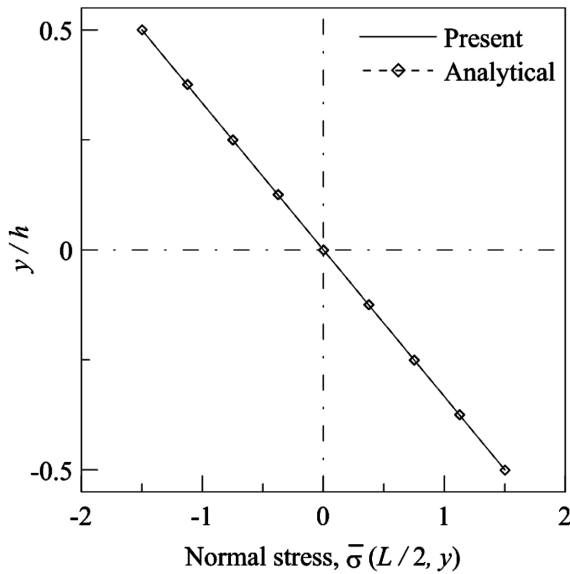
Fig. 5 Maximum normal stress distribution through the thickness of a simply supported isotropic beam (*L/h* = 100)
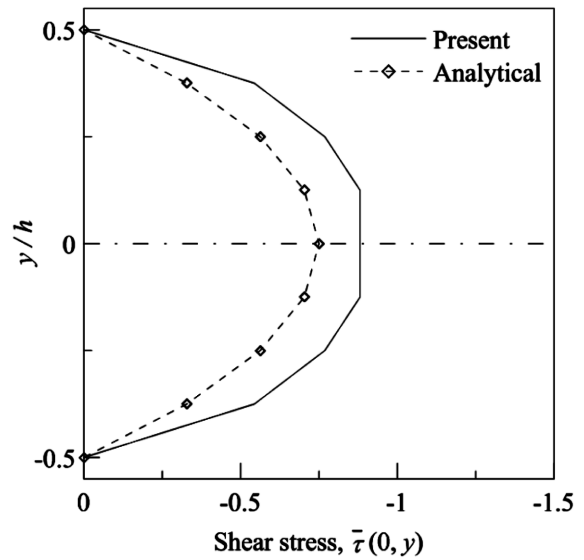

Fig. 6 Maximum shear stress distribution through the thickness of a simply supported isotropic beam (*L/h* = 100)

Table 2 Normalized natural frequencies $\overline{\omega}$ of a simply supported isotropic beam

n	*L/h* = 10			*L/h* = 20			*L/h* = 100		
	Modes	Present	Exact[1]	Modes	Present	Exact	Modes	Present	Exact
1	f(1)[2]	2.8024	2.8023	f(1)	2.8372	2.8371	f(1)	2.8487	2.8486
2	f(2)	10.7113	10.7087	f(2)	11.2121	11.2092	f(2)	11.3917	11.3887
3	e(1)	15.7080	-	f(3)	24.7586	24.7285	f(3)	25.6359	25.6030
4	f(3)	22.5854	22.5613	e(1)	31.4160	-	f(4)	45.6415	45.4628
5	f(4)	37.2520	37.1427	f(4)	42.9891	42.8350	f(5)	71.5818	70.9284
6	e(2)	47.1278	-	f(5)	65.4128	64.8882	f(6)	103.7953	101.9494
7	f(5)	53.8282	53.4968	f(6)	91.6148	90.2453	f(7)	142.7248	138.4650
8	f(6)	71.7441	70.9657	e(2)	94.2555	-	e(1)	157.0798	-
9	e(3)	78.5881		f(7)	121.2267	118.3125	f(8)	199.8832	180.4049
10	f(7)	90.6359	89.1205	f(8)	157.1762	148.5707	f(9)	248.1434	227.6894
11	f(8)	110.2042	107.6867	e(3)	160.4676	-	f(10)	315.4145	280.2307
12	e(4)	113.1898	-	f(9)	192.0240	180.5824	-	-	-
13	f(9)	131.4003	126.4893	f(10)	220.4084	213.9871	-	-	-
14	f(10)	142.1973	145.4163	-	-	-	-	-	-

[1]Analytical solution based on Timoshenko beam theory
[2]"f" and "e" indicate flexural and extensional modes, respectively.

through the thickness are used for stress distributions. The followings are employed for normalization

$$\bar{\sigma} = \frac{\sigma A h}{PL}, \quad \bar{\tau} = \frac{\tau A}{P} \tag{20}$$

Fig. 5 compares the normal stresses obtained by the present model and the analytical method based on the first-order shear theory. As seen in the figure, the present model is very successful to capture accurate normal stresses. Since the present model assumes the shear stress through the thickness is constant, more layers in vertical direction, i.e., *y*-direction, should be used to obtain better results. As seen in Fig. 6, the present model gives greater shear stress than that of the analytical solution.

Table 2 gives some lower natural frequencies of the isotropic simple beam for different *L/h*. Since the governing differential equations given by Eq. (1) include *u* and *v* variables, the present model yields both extensional and flexural vibration modes. For flexural vibration, results for natural frequencies of the present model are in good agreement with those of the exact solution.

Table 3 Normalized maximum deflections $\bar{v}$ for laminated composite beams under center point load

Laminate	*L/h*	Model	Boundary conditions[1]		
			H-H	C-C	C-F
0	10	Present	1.696	0.932	18.814
		Analytical[2]	1.600	0.850	18.400
	20	Present	1.176	0.424	16.707
		Analytical	1.150	0.400	16.600
	100	Present	1.007	0.257	16.028
		Analytical	1.001	0.256	16.024
90	10	Present	25.707	6.952	402.83
		Analytical	26.500	7.750	406.00
	20	Present	25.177	6.426	400.71
		Analytical	25.375	6.625	401.50
	100	Present	25.007	6.257	400.03
		Analytical	25.015	6.265	400.00
(0/90/90/0)	10	Present	1.809	0.949	20.890
		Analytical	1.991	1.141	21.578
	20	Present	1.306	0.452	18.861
		Analytical	1.348	0.498	19.006
	100	Present	1.143	0.291	18.209
		Analytical	1.143	0.292	18.184

[1]H – Hinged, C – Clamped, F – Free
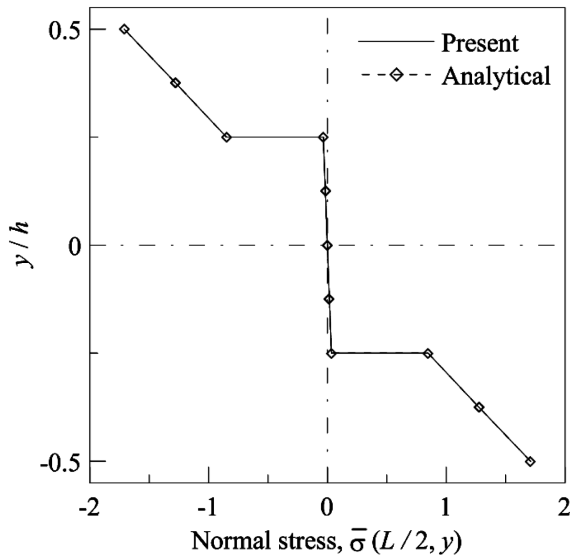[2]Analytical solution based on the first-order shear deformation theory (Reddy 1997)

Fig. 7 Normal stresses through the thickness of a simply supported (0/90/90/0) laminated beam ($L/h = 100$)
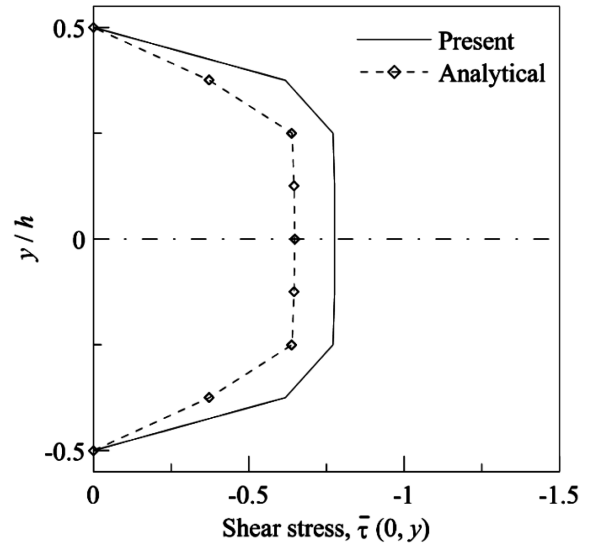

Fig. 8 Shear stresses through the thickness of a simply supported (0/90/90/0) laminated beam ($L/h = 100$)

Example 2 In the second example, laminated composite beams with different lamina lay-up under center point load are considered. Material properties are selected as $E_1/E_2 = 25$, $G_{12} = G_{13} = 0.5E_2$, $G_{23} = 0.2E_2$ and $v_{12} = 0.25$ (Reddy 1997). Table 3 shows normalized maximum deflections for different L/h and boundary conditions. As can be seen in the table, results of the present model agree well with the analytical solution based on the first-order shear theory by Reddy (1997).

In Figs. 7 and 8, the maximum normal and shear stress distributions through the thickness of a symmetrically laminated (0/90/90/0) composite beam with simple supports are given. Here, eight layers are used along the thickness for stress calculations. Similar to the isotropic beam, the present model has a good accuracy for normal stresses while giving greater shear stresses than the analytical solution based on the first-order shear theory.

Example 3 For further verification of the present multilayered beam element, natural frequencies of some laminated beams of which geometrical and material properties given in Table 4 are investigated. In Table 5, a comparison of the first nine natural frequencies for flexural vibration obtained by the present model with that of two-dimensional (2D) elasticity solution by Chen *et al.* (2003) is given. As can be seen, the present model is quite efficient to determine natural frequencies even for higher modes.

4.2 Moving load analysis results

Hereafter, results for dynamic response of some laminated composite beams on which a concentrated load P moves with a constant speed c are given. In the following figures, subscripts "*d*" and "0" indicate dynamic response and the maximum static response, respectively.

Example 4 Response of an isotropic simple beam to a moving load is first considered. Material

Table 4 Geometrical and material properties for Example 3 (Chen *et al.* 2003)

	Description	Data
Beam-1	Three-layer sandwich beam (face/core/face)	$L = 914.4$ mm, $b = 25.4$ mm, $h = 13.614$ mm Face layer: $h_f = 0.4572$ mm, $E_f = 68.97$ GPa, $v_f = 0.3$, $\rho_f = 2683$ kg/m³ Core layer: $h_c = 12.7$ mm, $G_c = 82.764$ GPa, $v_c = 0.3$, $\rho_c = 32.8381$ kg/m³
Beam-2	Five-layer sandwich beam (face/core/face/core/face)	$L = 508$ mm, $b = 25.4$ mm, $h = 21.844$ mm Face layer: $h_f = 0.508$ mm, $E_f = 68.97$ GPa, $v_f = 0.3$, $\rho_f = 1.0691 \times 10^7$ kg/m³ Core layer: $h_c = 10.16$ mm, $G_c = 34.485$ GPa, $v_c = 0.3$, $\rho_c = 2.6726 \times 10^6$ kg/m³
Beam-3	(0/90/90/0) laminated composite beam	$L = 381$ mm, $b = 25.4$ mm, $h = 25.4$ mm $E_1 = 145$ GPa, $E_2 = 9.6$ GPa, $G_{12} = 4.1$ GPa $v_{12} = 0.3$, $\rho = 1570$ kg/m³
Beam-4	(0/0/90/90/0/0) laminated composite beam	$L = 762$ mm, $b = 25.4$ mm, $h = 152.4$ mm $E_1 = 525$ GPa, $E_2 = 21$ GPa, $G_{12} = 10.51$ GPa $v_{12} = 0.3$, $\rho = 800$ kg/m³

Table 5 Natural frequencies of laminated beams with different end conditions for the first nine flexural modes

n	1	2	3	4	5	6	7	8	9
Beam-1 (H-H[1], f: Hz)									
Present	57.3049	218.1627	456.6918	745.1673	1057.4112	1422.6782	1762.2835	2152.8223	2481.4142
2D[2]	57.4837	220.7156	467.0315	770.4177	1108.9263	1467.2388	1827.5263	2256.9333	2617.5000
Beam-1 (C-F[3], f: Hz)									
Present	33.8998	197.8568	504.1749	884.6975	1306.7644	1683.0682	1749.1343	2200.5757	2648.4590
2D	33.958	199.857	513.561	907.979	1348.827	1682.761	1813.963	2320.409	2781.882
Beam-2 (H-H, ω_m: rad/sec)									
Present	10.5999	30.1984	50.3954	70.1759	90.6946	128.8924	149.1888	168.3866	188.8004
2D	10.9138	32.0618	54.2787	76.1316	97.6311	118.9123	139.6127	163.9236	176.0183
Beam-3 (C-C, $\overline{\omega}_n = \omega_n(L^2/h)\sqrt{\rho/E_1}$)									
Present	4.5910	10.3121	17.0435	24.2115	31.5990	-	-	-	-
2D	4.7120	10.7066	17.7965	25.3746	33.1948	-	-	-	-
Beam-3 (C-F, $\overline{\omega}_n$)									
Present	0.9215	4.8856	11.4463	17.1779	18.7495	26.3536	-	-	-
2D	0.9149	4.8820	11.3898	17.0673	18.4218	25.9372	-	-	-
Beam-4 (H-H, $\overline{\omega}_n$)									
Present	1.5556	3.8496	5.7396	7.8032	9.8686	11.9358	16.1612	18.2083	19.7571
2D	1.6591	3.9000	6.1342	8.3569	10.5728	12.7663	14.9832	17.2059	19.2723

[1]H - Hinged, C - Clamped, F - Free
[2]Semi-analytical solution based on 2D elasticity (Chen *et al.* 2003)
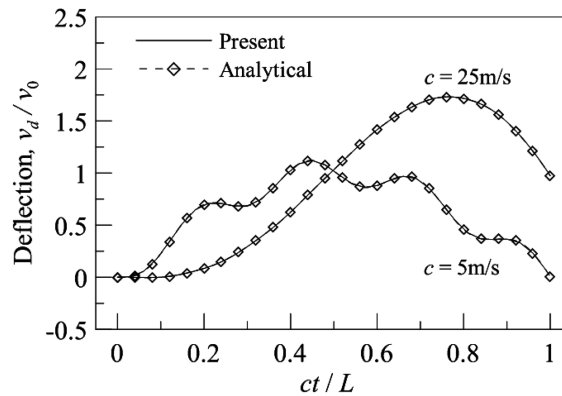[3]For this cantilever beam, $L = 711.2$ mm is taken as in Chen *et al.* (2003).

Fig. 9 Normalized maximum deflections of a simple isotropic beam when the load moves on the beam ($L/h = 100$)
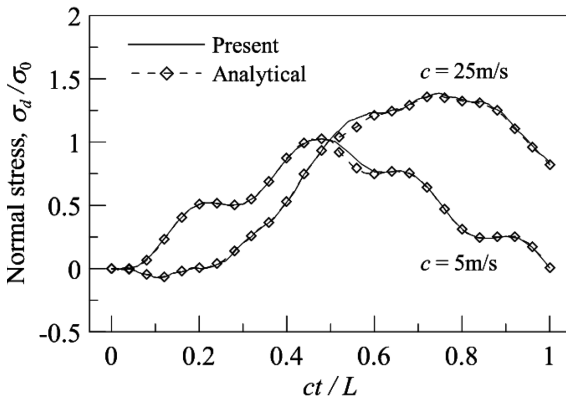

Fig. 10 Normal stress distribution for a simple isotropic beam when the load moves on the beam ($L/h = 100$)
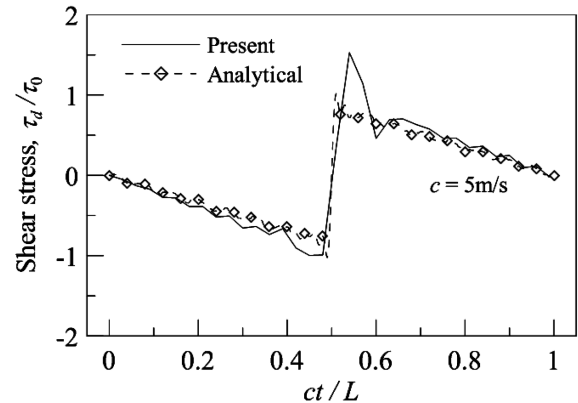

Fig. 11 Shear stress distribution for a simple isotropic beam when the load moves on the beam ($L/h = 100$)

properties were given in Example 1. Analytical solutions are obtained by the assumed mode method for 100 modes. In Fig. 9, dynamic deflections at midpoint, which are normalized by the maximum static deflection, are given when the load moves along the beam length with speeds of 5 m/s and 25 m/s. The critical speed for this beam is calculated as $c_{cr} = \omega_1 L/\pi = 39.88$ m/s. As seen in the figure, the present model shows perfect agreement with the analytical solution.

Figs. 10 and 11 show the normal stress at $y = -h/2$ (bottom) and the shear stress at $y = 0$ (center) at midspan of the beam when the load moves on the beam. Both normal and shear stresses are normalized by the maximum stresses occurring in the beam for static loading. As seen in the figures, the results of the present model agree well with those of the analytical solution.

Example 5 In this example, dynamic behavior of laminated composite beams under a moving point load is considered. A comparison between the steel and laminated composite beams is made through Figs. 12 to 14 in terms of the dynamic magnification factors (*DMF*) of deflections, normal and shear stresses. *DMF* is defined as the ratio of maximum dynamic response at midspan to the
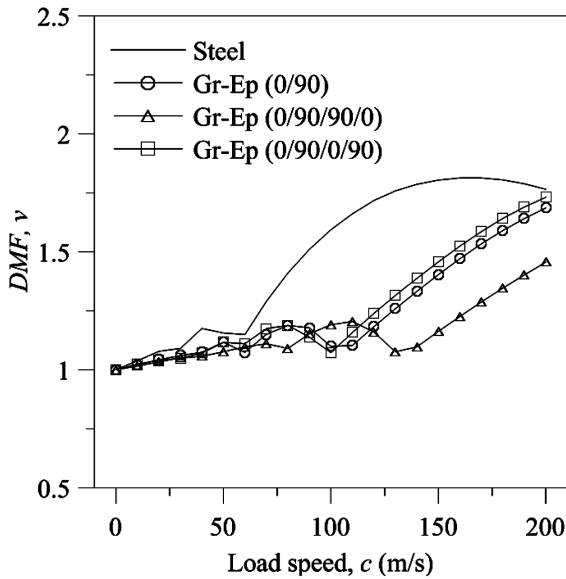
Fig. 12 Comparison of dynamic magnification factors of deflection for steel and graphite-epoxy composite beams
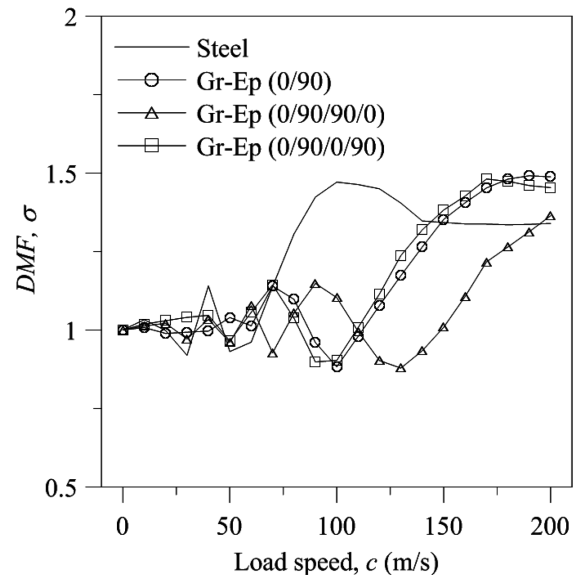

Fig. 13 Comparison of dynamic magnification factors of normal stress for steel and graphite-epoxy composite beams
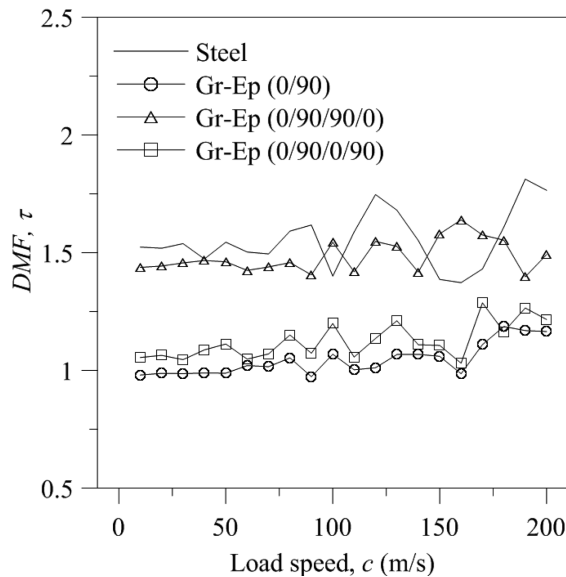

Fig. 14 Comparison of dynamic magnification factors of shear stress for steel and graphite-epoxy composite beams

maximum static response. Material properties are selected as given in Example 1 for steel and as Beam-3 in Table 4 for graphite-epoxy composite. While beam length $L = 381$ mm and width $b = 25.4$ mm are kept constant, beam height is changed to have same static deflection at midpoint under

center point load for the beams considered. According to static analysis results, $h = 25.4$ mm for steel beam, $h = 48.26$ mm for graphite-epoxy (0/90) beam, and $h = 31.75$ mm for graphite-epoxy (0/90/90/0) beam yield approximately same midpoint deflection. (0/90/0/90) laminated beam is selected to study the effect of lamina stacking on the beam response.

According to Fig. 12, laminated composites generally show better deflection behavior than the steel beam especially for higher load speeds. The unsymmetrical (0/90) and (0/90/0/90) laminates give approximately same deflections but thickness of (0/90/0/90) laminate is 35% less than that of (0/90) laminate. The (0/90/90/0) laminate has the best behavior in terms of the dynamic deflections compared to the others. Similar results are also obtained for normal stresses as seen in Fig. 13. In Fig. 14, one can observe the unsymmetrical (0/90) and (0/90/0/90) laminated beams show better dynamic behavior regarding shear stresses. Fig. 14 also show the (0/90/90/0) laminate has better shear stress behavior than the steel beam. Regarding to the effect of lamina stacking on the response, symmetrical laminated beams are better than unsymmetrical ones as seen in Figs. 12 to 14.

5. Conclusions

A multilayered beam element for static and dynamic analyses of laminated beams based on the first-order shear deformation theory is presented. While this element allows separate rotational degrees of freedom for each lamina, it does not require any additional axial and transversal degrees of freedom beyond those necessary for a single lamina. Comparisons with the results available in literature demonstrate the accuracy of present element in terms of deflections, stresses and natural frequencies of laminated beams. Regarding moving load-induced dynamic response, composite laminates are better than the steel beam especially for high-speeds. Results also show that unsymmetrical laminates give smaller dynamic shear stresses. According to results of this study, use of composite laminates in structural applications allows us to achieve more effective systems in terms of weight and strength.

References

Abu-Hilal, M. and Mohsen, M. (2000), "Vibration of beams with general boundary conditions due to moving harmonic load", *J. Sound Vib.*, **232**, 703-717.

Au, T.K., Cheng, Y.S. and Cheung, Y.K. (2000), "Vibration analysis of bridges under moving vehicles and trains: an overview", *Progr. Struct. Eng. Mater.*, **13**, 299-304.

Bassiouni, A.S., Gad-Elrab, R.M. and Elmahdy, T.H. (1999), "Dynamic analysis for laminated composite beams", *Compos. Struct.*, **44**, 81-87.

Cantero, D., O'Brien, E.J. and González, A. (2010), "Modelling the vehicle in vehicle–infrastructure dynamic interaction studies", *Proceedings of the Institution of Mechanical Engineers, Part K: Journal of Multi-body Dynamics*, **224**, 243-248.

Chen, W.Q., Lv, C.F. and Bian, Z.G. (2003), "Elasticity solution for free vibration of laminated beams", *Compos. Struct.*, **62**, 75-82.

Chonan, S. (1975), "The elastically supported Timoshenko beam subjected to an axial force and a moving load", *Int. J. Mech. Sci.*, **17**, 573-581.

Frýba, L. (1999), *Vibration of Solids and Structures under Moving Loads*, 3rd Editions, Thomas Telford Ltd., Prague.

Ghafoori, E. and Asghari, M. (2010), "Dynamic analysis of laminated composite plates traversed by a moving mass based on a first-order theory", *Compos. Struct.*, **92**, 1865-1876.

Hino, J., Yoshimura, T., Konishi, K. and Ananthanarayana, N. (1984), "A finite element method prediction of the vibration of a bridge subjected to a moving vehicle load", *J. Sound Vib.*, **96**, 45-53.

Kadivar, M.H. and Mohebpour, S.R. (1998), "Finite element dynamic analysis of unsymmetric composite laminated beams with shear effect and rotary inertia under the action of moving loads", *Finite Elem. Anal. Des.*, **29**, 259-273.

Kahya, V. (2012), "Dynamic analysis of laminated composite beams under moving loads using finite element method", *Nucl. Eng. Des.*, **243**, 41-48.

Kahya, V. and Mosallam, A.S. (2011), "Dynamic analysis of composite sandwich beams under moving mass", *KSU J. Eng. Sci.*, **14**, 18-25.

Kavipurapu, P.K. (2005), "Forced vibration and hygrothermal analysis of composite laminated beams under the action of moving loads", M.Sc. Thesis, Morgantown, West Virginia University.

Kiral, B.G., Kiral, Z. and Baba, B.O. (2004), "Dynamic behavior of laminated composite beams subjected to a moving load", *J. Appl. Sci.*, **4**, 271-276.

Kocatürk, T. and Şimşek, M. (2006), "Dynamic analysis of eccentrically prestressed viscoelastic Timoshenko beams under a moving harmonic load", *Comput. Struct.*, **84**, 2113-2127.

Lee, S.Y., Yhim, S.S. (2004), "Dynamic analysis of composite plates subjected to multi-moving loads based on a third order theory", *Int. J. Solids Struct.*, **41**, 4457-4472.

Malekzadeh, P., Fiouz, A.R. and Razi, H. (2009), "Three-dimensional dynamic analysis of laminated composite plates subjected to moving load", *Compos. Struct.*, **90**, 105-114.

Mohebpour, S.R., Fiouz, A.R. and Ahmadzadeh, A.A. (2011), "Dynamic investigation of laminated composite beams with shear and rotary inertia effect subjected to the moving oscillators using FEM", *Compos. Struct.*, **93**, 1118-1126.

Mohebpour, S.R., Malekzadeh, P. and Ahmadzadeh, A.A. (2011), "Dynamic analysis of laminated composite plates subjected to a moving oscillator by FEM", *Compos. Struct.*, **93**, 1574-1583.

Reddy, J.N. (1997), *Mechanics of Laminated Composite Plates: Theory and Analysis*, CRC Press, New York.

Şimşek, M. and Kocatürk, T. (2009), "Nonlinear dynamic analysis of an eccentrically prestressed damped beam under a concentrated moving harmonic load", *J. Sound Vib.*, **320**, 235-253.

Yang, Y.B., Yau, J.D. and Wu, J.S. (2004), *Vehicle-Bridge Interaction Dynamics with Applications to High-Speed Railways*, World Scientific Publishing, Singapore.

Yuan, F.G. and Miller, R.E. (1989), "A new finite element for laminated composite beams", *Comput. Struct.*, **31**, 737-745.

Yuan, F.G. and Miller, R.E. (1990), "A higher-order finite element for laminated beams", *Comput. Struct*, **14**, 125-150.

Zibdeh, H.S. and Abu-Hilal, M. (2003), "Stochastic vibration of laminated composite coated beam traversed by a random moving load", *Eng. Struct.*, **25**, 397-404.

Zienkiewicz, O.C. and Taylor, R.L. (2000), *The Finite Element Method: The Basis*, Vol. 1, 5th Editions, Butterworth-Heinemann, Oxford.

Appendix

Elements of **H** matrix are given in the following.

$$\mathbf{H} = \begin{bmatrix}
-\dfrac{3E}{L_e} & \dfrac{4E}{L_e} & -\dfrac{E}{L_e} & 0 & 0 & 0 & 0 & \dfrac{3Eh}{2L_e} & -\dfrac{2Eh}{L_e} & \dfrac{Eh}{2L_e} \\[2ex]
-\dfrac{3E}{L_e} & \dfrac{4E}{L_e} & -\dfrac{E}{L_e} & 0 & 0 & 0 & 0 & \dfrac{3Eh}{2L_e} & \dfrac{2Eh}{L_e} & -\dfrac{Eh}{2L_e} \\[2ex]
0 & 0 & 0 & -\dfrac{11G}{2L_e} & \dfrac{9G}{L_e} & -\dfrac{9G}{2L_e} & \dfrac{G}{L_e} & -G & 0 & 0 \\[2ex]
\dfrac{E}{L_e} & -\dfrac{4E}{L_e} & \dfrac{3E}{L_e} & 0 & 0 & 0 & 0 & -\dfrac{Eh}{2L_e} & \dfrac{2Eh}{L_e} & -\dfrac{3Eh}{2L_e} \\[2ex]
\dfrac{E}{L_e} & -\dfrac{4E}{L_e} & \dfrac{3E}{L_e} & 0 & 0 & 0 & 0 & \dfrac{Eh}{2L_e} & -\dfrac{2Eh}{L_e} & \dfrac{3Eh}{2L_e} \\[2ex]
0 & 0 & 0 & -\dfrac{G}{L_e} & \dfrac{9G}{2L_e} & -\dfrac{9G}{L_e} & \dfrac{11G}{2L_e} & 0 & 0 & -G
\end{bmatrix} \tag{A1}$$

where L_e is the element length.